FACTORS CONTROLLING POLYGON SIZES IN THE MARTIAN NEAR-SURFACE.
B. J. Travis[1] and W. C. Feldman[2], [1]Computational Earth Science Group, EES-16/MS-T003, Los Alamos National Laboratory, Los Alamos, NM 87545, bjtravis@lanl.gov, [2]Planetary Science Institute, Tucson, AZ, feldman@psi.edu.

Introduction: Polygonal ground on Mars is widespread [1, 2, 3] and is seen generally at high northern latitudes [4], in Athabasca Valles, Elysium basin, Marte Vallis, western Amazonis Planitia, as well as the Cerberus Fossae region [5, 6]. At many sites, polygon diameters range roughly from a few up to 20 meters or more (Figure 1), in agreement with sizes that have been shown to result from thermal contraction in ice-rich permafrost [3, 5]. Polygons are also frequently observed near stone circles, another feature of periglacial activity [7]. Sorted patterned ground on Earth results from freeze-thaw cycling and cryoturbation.

Hydrothermal circulation of brines in the near-surface of Mars is a mechanism that can deposit ice, and brine, close to, or even at, the surface of Mars [9]. Freezing and thawing patterns associated with brine convection also produce surface features such as polygonal ground with mounds and troughs, with polygon sizes similar to observed [9]. In this study, numerical simulations of brine convection in cold soil with resulting heaving/slumping of soil are compared to observations of Martian polygons. Factors affecting polygon sizes in brine convection include soil permeability, geothermal heat flux and pore water salt concentration.

Model: Previous experimental and numerical studies [8, 9] considered salty aquifer dynamics in response to a geothermal gradient under a freezing surface. Some salts, such as $CaCl_2$ and some ferric chlorides, can depress freezing points by 50 to 70 ^oC. Salt not only depresses the freezing point but can add an unsteady characteristic to hydrothermal convection [8]. Simulations reported here make use of the MAGHNUM code. MAGHNUM solves the time-dependent governing equations for water and vapor flow, and heat and salt transport in cold, porous, permeable media in 1-D, 2-D or 3-D geometries. It allows transformations between liquid, vapor and ice phases, depending on local thermodynamics. Thermal conductivity and specific heat are re-computed on each time step in each computational cell by a volume fraction-weighted average of the thermal conductivities and specific heats of soil, water, ice and air, each of which is temperature dependent. Chemical, as well as thermal, buoyancy is an important factor in driving flow. Fluid density ρ_f is a function of temperature T and salt content C. Fluid viscosity depends on temperature and salt content, and is based on experimental data [8]. At the eutectic, fluid viscosity is more than an order of magnitude greater than for pure water above freezing. Salt precipitation and dissolution are computed by partitioning salt between fluid and solid phases according to the binary phase graph for $CaCl_2$ and H_2O.

Surface Deformation: Freezing of water results in a volume change, which in turn, leads to either heaving of soil (upon freezing) or slumping (due to melting of ice). We have estimated the surface deformation, that is, spatial distribution of elevation change, due to the spatial pattern of subsurface ice formation in our model simulations, by integrating volume change over depth, that is,

$$\Delta z(x) = \int i(x,z)\, \varepsilon(x,z)\, (\rho_w - \rho_i)/\rho_w \, dz$$

where Δz is the local surface elevation (compared to an unfrozen soil), $i(x,z)$ is the local ice fraction, $\varepsilon(x,z)$ is local porosity, ρ_i and ρ_w are ice and water densities. Model domains are 200x100 m for 2-D (x-z) cases and 200x200x100 m for 3-D simulations.

Simulations consider a range of permeabilities (10-1000 darcies), geothermal heat fluxes (20-80 mW/m^2) and initial salt contents (5-30%wt); surface temperature is -52 ^oC for most cases, the eutectic temperature of $CaCl_2$.

Results: Table 1 summarizes a number of simulations. Variables listed are the soil permeability Perm, in darcies, Q the geothermal heat flux in mW/m^2, C_{in}, the pore water salt concentration % mass, W, the average polygon diameter (m), D, the average depth (m) of troughs surrounding polygons, and UPL, the average uplift (m) of polygon centers. Generally, average uplift is about 0.2 m, with small variations. A general result is that margins and troughs are typically deeper than mounds are high. Troughs show greater variability in depth. Mounds overlie ice lenses in the upwelling regions, while troughs overlie downwellings that are ice-poor. The elevation difference between mound height and the surrounding trench depression is roughly 0.35 m to as much as 1.50 m. The sizes of model polygons at the surface show wide variability, from 5 m to 60+ m. Based on simulation results, permeability and bulk salt content are the two most important variables. Higher salt content leads to more well-defined polygon features and greater variability in polygon diameters. Low bulk salt content corresponds to higher central mounds and smaller diameters. Detailed 3-D simulations show Rayleigh-Taylor (R-T) instabilities in troughs. These are weak at high salt concentrations, but at low bulk salt concentrations, the R-T instabilities dominate the flow pattern, resulting in shallow troughs dotted with many isolated deeper pits about the size of the small boulders seen in Figure 1.

References: [1] Mangold N. S. et al (2004) *JGR 109,* E08001. [2] Mangold N. S. (2005) *Icarus, 174,* 336-359. [3] Levy J. et al (2009) *JGR 114*, E01007. [4] Mellon M. T. et al (2008) *JGR 113,* E00A23. [5] Mellon M. T. (1997) *JGR, 102*, 25617-25628. [6] Page D. P. and Murray J. B. (2006) *Icarus 183,* 46-54. [7] Balme M. R. and Gallagher C. (2009) *EPSL,* doi:10.1016 /j.epsl.2009.05.031. [8] McGraw et al (2006) *LPS XXXVII*, 2224. [9] Travis, B. J. et al (2013) *JGR Planets, 118*, doi: 10.1002/jgre.20074.

Table 1 Modeled Polygon Features

Case	Perm	Q	Cin	W	D	UPL
1	100	40	29	67	0.27	0.12
2	10	40	29	50	0.01	0.01
3	1000	40	29	20	0.18	0.07
4	100	40	25	50	0.80	0.25
5	100	40	20	40	1.52	0.28
6	100	30	29	33	0.22	0.08
7	100	60	29	40	0.26	0.09
8*	100	40	20	28	0.72	0.31
9#	100	40	29	67	0.01	0.005
10*	100	40	29	33	0.17	0.07
11	100	40	10	33	0.81	0.23
12	100	40	5	15	0.30	0.17

* = surface temperature is -50 ^oC
# = surface temperature is -54 ^oC

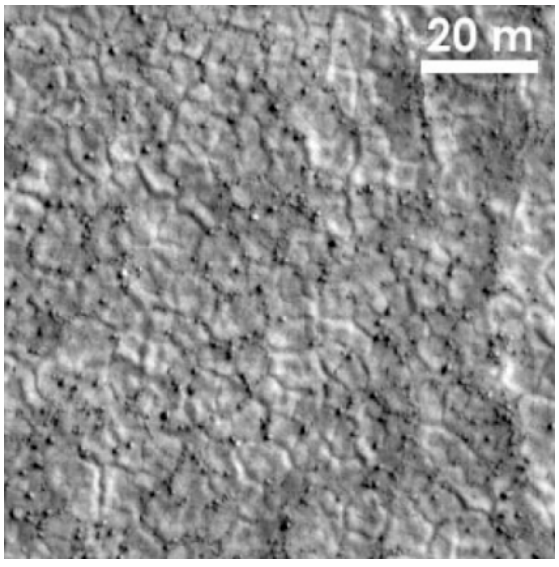

Figure 1 Example of patterned ground. HiRISE PSP-001381-2485. Individual rocks can be seen, tending to collect in troughs that define the edges of polygons. Image courtesy of M. T. Mellon.